Robotica (2001) volume 19, pp. 199–207. Printed in the United Kingdom © 2001 Cambridge University Press

Random execution of a set of contacts to solve the grasping and contact uncertainties in robotic tasks

Alvin Chua, Jayantha Katupitiya and Joris De Schutter

Mechanical Engineering Department, De La Salle University, 2401 Taft Avenue, Manila 1004 (Philippines)

(Received in Final Form: June 29, 2000)

SUMMARY

This paper addresses the problem of identifying the uncertainties present in a robotic contact situation. These uncertainties are errors and misalignments of an object with respect to its ideal position. The paper describes how to solve for the errors caused during grasping and errors present when coming into contact with the environment. A force sensor is used together with Kalman Filters to solve for all the uncertainties. The straightforward use of a force sensor and the Kalman Filters is found to be effective in finding only some of the uncertainties in robotic contact. The other uncertainties form dependencies that cannot be estimated in this manner. This dependency brings about the problem of *observability.* To make the unobservable uncertainties observable a sequence of contacts are used. The error covariance matrix of the Kalman Filter (KF) is used to obtain new contacts that are required to solve for all the uncertainties completely. There is complete freedom in choosing which unobservable quantity to be excited in forming the next contact. The paper describes how these new contacts can be randomly executed. A two dimensional contact situation will be used to demonstrate the effectiveness of the method. Experimental data are also presented to prove the validity of the procedure. Due to the non-linear relationship between the uncertainties and the forces, an Extended Kalman Filter (EKF) has been used.

KEYWORDS: Kalman filters; Optimal estimation; Identification; Observability.

1. INTRODUCTION

In robotic part mating, the identification and compensation of uncertainties (errors and misalignments of objects) are very important for successful assembly. The uncertainties present belong to two categories: grasping and contact uncertainties. The *grasping uncertainties* are the uncertainties in the geometric configuration that deviates from the ideal grasping condition. The *contact uncertainties* are those that arise due to unknown contact with the environment. Under the contact uncertainties, there is the topological and the geometrical uncertainties. The *geometrical uncertainties* pertain to the unknown position and orientation of the grasped object with respect to the environment. While the *topological uncertainties* refer to the number of contacts and the type of each contact.[1,2] In this paper, we will be interested in the identification of geometrical contact uncertainties and, grasping uncertainties (See Fig. 1). We will also include the ever present but usually neglected effect of friction in the contact situation. To do this, we introduce a friction angle uncertainty, which will take into account the effect of friction in the contact situation.

The use of a force sensor as a feedback sensor in assembly operations is widely accepted.[3] The guarded move and the stiffness matrix methods are among the simplest type of force feedback strategies.[4] The guarded move uses the force sensor to monitor a certain threshold value of force and the stiffness matrix method relates the stiffness to displacement. Another method used to extract information from the force sensor is the centre of overlap strategy.[5] Also, Qiao[5] used a procedural technique using force sensor measurements to find its way in a peg-hole insertion problem. It is based on the assumption that a peg to be inserted lies within a quadrant of the hole. Other studies using a force sensor are found in papers.[6–8] This study uses a force sensor to gather data, which will be used in a KF to estimate the uncertainties of a robotic contact for an unhindered progress of the assembly task.

The straightforward identification process using the KF is complicated by the presence of unobservable quantities. The problem of observability stems from the fact that certain uncertainties form dependencies. The problem of observability exists in systems when the state of the system cannot be uniquely determined from past observations.[9] For a linear system to be observable, the observability matrix should have its rank equal to the dimension of the state vector. For a nonlinear case, two sufficient conditions of global observability are used, namely: the ratio condition and the strongly positive semi-definition condition.[10] Other papers[11–13] give different criteria for detection of observability in different applications. In reference [1], the information about the state observability was obtained by taking Singular Value Decomposition of the error covariance matrix. The dependency of the uncertainties was solved using the error covariance matrix and the geometric relationship between contact situations. This would provide a smooth progression from one contact situation over to the other.

When the object comes in contact with the environment, due to the presence of the compliance, the object held in the gripper will undergo forces as well as displacements with respect to the end effector. The forces are expressed with a wrench vector and the displacements are expressed with a

https://doi.org/10.1017/S0263574700002903 Published online by Cambridge University Press

twist vector. In this study only the wrench vector is used. The twist vector is not used because of the complexity involved in measuring it. However, every attempt has been made to keep the twist vector to a minimum (by using lower compliances and lower forces) so that the absence of twist vector will not cause excessive errors in the final solution.

The method described here can be viewed as an active sensing strategy. This means that the sensing (collecting force data) will continue based on the error covariance matrix until all uncertainties including friction are completely determined. The identification of friction is very important since it has a lot of variation in different environments.

The KF can be used to estimate a stationary state vector (a state vector that is not changing) or a non-stationary (evolving) state vector. To estimate evolving state vectors, a state transition matrix representing system dynamics must be used and the sampling time plays an important role. In this paper, the KF is used to estimate a stationary vector. This is because, in a given contact situation, the uncertainties do not change. Further, the KF can be used in three different modes. They are: (a) as an estimator for the off-line processing of data gathered earlier, (b) as a filter to improve the current estimate based on the measurement data just received and (c) as a predictor to predict the state vector at some future instant.[14] In this paper, the KF is used as an estimator. Once a contact has been established, a sufficient number of force data is gathered. During the acquisition of force data no Kalman Filtering is carried out. In our experiments we took 200 force data readings at each contact situation with a sampling time of 5 ms (as part of the robot control interrupt service routine). However, the sampling time plays no role as we are using the KF as an estimator to estimate a stationary uncertainty vector. Once data has been gathered, the robot is halted until the KF processes the data. The halt time is about 400 ms with the KF running as a foreground process of the same 486DX2–66 computer. As can be seen, the halt period is insignificant in a practical assembly situation.

2. EXTENDED KALMAN FILTER

Kalman filtering (KF) is one of the most common optimal filtering techniques for estimating parameters of linear systems. The identification is possible due to the relationship between the state variables and the measurement data, which could come from any sensor that could be used to observe the system. Since the relationship between the measurement data and the uncertainties in our application is non-linear, the Extended Kalman Filter (EKF) is used. Using the notation given in Gelb,[3] the measurement model is represented by the equation

$$\boldsymbol{z}_k = \boldsymbol{h}_k(\boldsymbol{x}(t_k)) + \boldsymbol{\nu}_k; \quad k = 1, 2, \ldots; \quad \boldsymbol{\nu}_k \sim N(0, R_k) \tag{1}$$

$\boldsymbol{z}_k$ is the measurement vector, $\boldsymbol{h}_k$ is the measurement model, $\boldsymbol{x}(t_k)$ is the system state vector (consisting of uncertainties), and $\boldsymbol{\nu}_k$ is the additive measurement error. Based on every new measurement vector the existing estimate of the uncertainty is updated using

$$\hat{\boldsymbol{x}}_k(+) = \hat{\boldsymbol{x}}_k(-) + \boldsymbol{K}_k[\boldsymbol{z}_k - \boldsymbol{h}_k(\hat{\boldsymbol{x}}_k(-))] \tag{2}$$

In these equations, $(-)$ indicates quantities before the current measurement, $\boldsymbol{z}_k$, has been used and $(+)$ indicates the same quantities after $\boldsymbol{z}_k$ has been used. The Kalman gain matrix, $\boldsymbol{K}_k$ is given by,

$$\boldsymbol{K}_k = \boldsymbol{P}_k(-)\boldsymbol{H}_k^T(\boldsymbol{x}_k(-)) \left[\boldsymbol{H}_k(\hat{\boldsymbol{x}}_k(-))\boldsymbol{P}_k(-)\boldsymbol{H}_k^T(\hat{\boldsymbol{x}}_k(-)) + \boldsymbol{R}_k\right]^{-1} \tag{3}$$

where the H-matrix is found by taking the derivative of the measurement model with respect to each state variable.

$$\boldsymbol{H}_k(\hat{\boldsymbol{x}}(-)) = \frac{\partial \boldsymbol{h}_k(\boldsymbol{x}(t_k))}{\partial \boldsymbol{x}(t_k)}\Big|_{x(t_k)=\hat{x}(-)} \tag{4}$$

The Error Covariance matrix or $\boldsymbol{P}$-matrix is found by using the equation below. By assuming a certain error of the first guess, after a sufficient number of iterations the KF can find a very close estimate of the state vector.

$$\boldsymbol{P}_k(+) = [\boldsymbol{I} - \boldsymbol{K}_k\boldsymbol{H}_k(\hat{\boldsymbol{x}}_k(-))]\boldsymbol{P}_k(-) \tag{5}$$

For a comprehensive discussion of the KF, refer to Gelb[14] and Bar-Shalom.[15]

3. STRATEGY TO SOLVE THE UNOBSERVABLE UNCERTAINTIES

In our application, the KF output provides the following types of information: (a) the uncertainties that are fully determined (as indicated by zero or close to zero diagonal elements of $\boldsymbol{P}_k(+)$), (b) the uncertainties that were unable to be determined (as indicated by non-zero diagonal elements of $\boldsymbol{P}_k(+)$), (c) the uncertainties that form dependencies (as indicated by the non-zero off-diagonal elements of $\boldsymbol{P}_k(+)$). The approach presented here forms a close resemblance to closed-loop calibration method.[16–18] The difference is that we use the KF to identify the dependencies (the unobservable uncertainties that form relationships – see eqns. (6)–(9)). As we go from one contact to another, the dependency information is carried forward. Thus the result of a contact situation that forms a dependency is not discarded.

In most practical situations the uncertainties are known to lie within limits. This can be used as the *a priori* estimate in the KF. It also allows us to form a sensible initial value for the $\boldsymbol{P}$ matrix. The gathered data allows us to input the correct values for the $\boldsymbol{R}$ matrix. Further, in assembly operations, some form of compliant motion takes place and most of the time active force control is implemented. Therefore it is natural to use the force sensor as the observer to obtain the $\boldsymbol{z}$ vector in eqn. (1). The direction of the new contact will be chosen randomly from among the directions of the unobservable quantities. In each of the new random contact situations, a transformation is used to relate the estimate obtained from the previous contact to suit the next contact.[1] The error covariance matrix is also updated to suit the new contact configuration. This procedure is carried out repeatedly until the complete solution is found.

4. ALGORITHM

Let m denote a given contact situation. Having gathered the force data, work out the covariance matrix $\boldsymbol{R}^m$. Knowing the

https://doi.org/10.1017/S0263574700002903 Published online by Cambridge University Press

ranges of uncertainties, an initial guess $\hat{\boldsymbol{x}}^m(-)$ and an initial value for the estimation error covariance $\boldsymbol{P}^m(-)$ can be obtained. At the end of the KF run, we obtain, $\boldsymbol{P}^m(+)$ and $\hat{\boldsymbol{x}}^m(+)$. If,

$$\boldsymbol{P}_{ii}^m(+) = 0 \tag{6}$$

then the i^{th} uncertainty is completely determined. If,

$$\boldsymbol{P}_{ii}^m(+) \neq 0 \tag{7}$$

then i^{th} uncertainty is unobservable. For the same i, if,

$$\boldsymbol{P}_{ij}^m(+) \neq 0; \quad (\boldsymbol{i} \neq \boldsymbol{j}) \tag{8}$$

then the i^{th} uncertainty has a dependency relationship with j^{th} uncertainty. A contact change must be carried out that will cause a change in the forces due to an unobservable uncertainty. Any $\hat{x}_i^m(+)$, that corresponds to i, satisfying eqn (7) can be randomly chosen to be changed to form the next contact. The order of choosing these uncertainties does not cause divergence. This paper emphasizes this fact. In general, maximum, possible change must be carried out to achieve a significant excitation. Note that, changing $\hat{x}_i^m(+)$ does not change the uncertainty associated with $\hat{x}_i^m(+)$. Since the robot carries out a known change, the transformation $\boldsymbol{T}_{\boldsymbol{m}}^{\boldsymbol{m+1}}$ between the state vector at contact m and $m+1$ can be established. Transform the current $\boldsymbol{P}^m(+)$ and $\hat{\boldsymbol{x}}^m(+)$ to obtain $\boldsymbol{P}^{m+1}(-)$ and $\hat{\boldsymbol{x}}^{m+1}(-)$ as follows:

$$\begin{aligned} \hat{\boldsymbol{x}}^{m+1}(-) &= \boldsymbol{T}_m^{m+1}\hat{\boldsymbol{x}}^m(+) \\ \boldsymbol{P}^{m+1}(-) &= \boldsymbol{T}_m^{m+1}\hat{\boldsymbol{x}}^m(+)\,\boldsymbol{T}_m^{\prime m+1} \end{aligned} \tag{9}$$

5. IMPLEMENTATION

To demonstrate the procedure, a 2-D set-up is shown in Figure 1. At the top of this figure, an end effector, a force sensor and a gripper are shown. The position of these three are assembled to be known. The rectangle in solid line, below the gripper is a cylindrical peg. As shown, the gripper does not properly grasp it. Although how the gripper is gripping the peg is not shown it is assumed that the gripper somehow grasps the peg in the position shown. The bottom most point of the improperly grasped peg is in contact with a surface. The surface is shown with a solid line. All the uncertainties associated with this situation are shown in the figure. They are, F, y, z, α, β and γ.

To show the validity of the procedure, two random contact sequences are considered. First, simulation results will be presented. Then, experimental results are given.

The first random contact sequence implemented to find the uncertainties is described below. When the grasped object makes the first contact with the surface, all uncertainties are unknown. The KF processes the force signals gathered during this contact. The final P-matrix showed a number of observable uncertainties and a number of unobservable uncertainties. The observable uncertainties are the force (F), the horizontal displacement error (y) and the vertical displacement error (z). The unobservable uncertainties are the contact angle between the grasped object and the surface (α), the grasping angle error (β), and the frictional angle (γ).

The uncertainties corresponding to the independent directions are fully determined where as the uncertainties corresponding to the dependent directions are not determined. Instead a dependency is determined in these directions. Out of the dependent uncertainties shown by the final P-matrix, a direction will be randomly chosen to carry out an end effector movement to establish a new contact. In this case the direction of β is chosen. The change in β is achieved by rotating the grasped object through 180 degrees about the gripper axis and making a new contact (second contact, look at Figure 2). Using the method described in

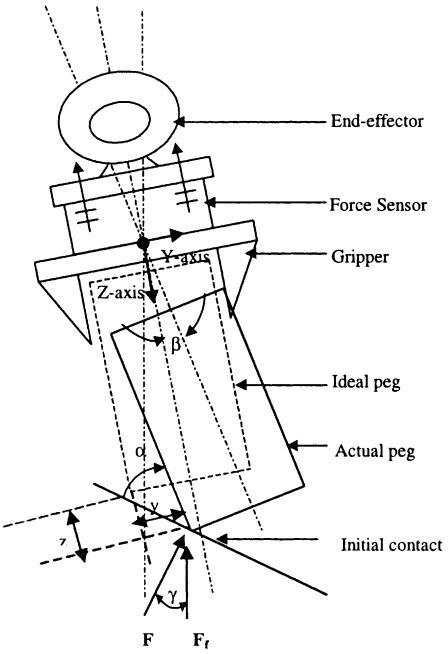

Fig. 1. Initial Peg-surface contact model.

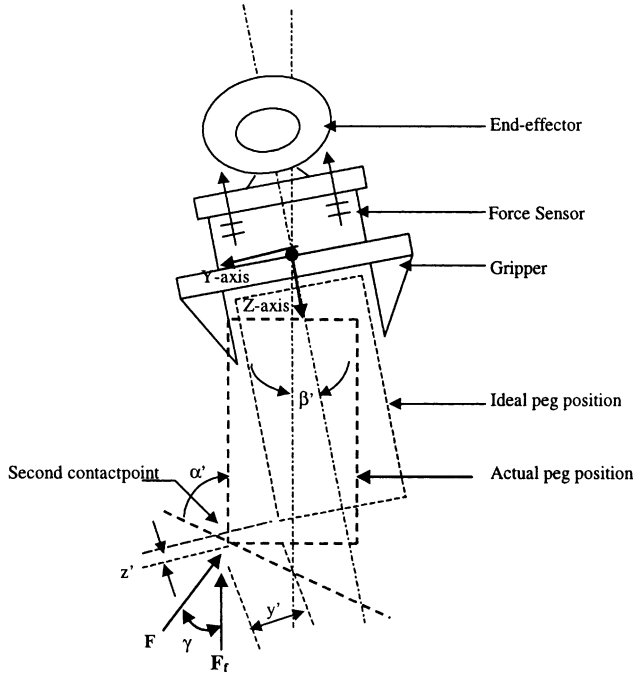

Fig. 2. 180° Rotation of the Initial Peg-surface contact model.

https://doi.org/10.1017/S0263574700002903 Published online by Cambridge University Press

reference [1], the final results of the KF run for the first contact is transformed to suit the Kalman Filtering to be done during the contact just established. The forces gathered during the second contact are then processed again using the KF. The final P-matrix of the second KF run indicated the remaining dependent uncertainties. At this stage, the direction of α is randomly chosen to carry out a contact change. A known change in α is then applied and a third contact is established. The forces gathered during the third contact were then processed by the KF. The final P-matrix then showed zero covariances with respect to β. This indicates that the uncertainty β has been completely determined. However, the same P-matrix showed dependencies between α and γ. This dependency could be solved by choosing the direction of γ. A change in γ can be achieved by carrying out a reverse movement. When the forces gathered during the reverse movement are processed, the KF gave a final P-matrix with all elements close to zero. This indicated the completion of the process to determine all the uncertainties.

The second random contact sequence consisted of the following four contact situations. The first is the initial contact situation as in the sequence described in the last paragraph with all uncertainties unknown. This was followed by the second contact based on the direction of γ chosen randomly from the dependent uncertainties shown by the final P-matrix of the KF. The next contact was established by choosing the direction of β. This choice is randomly made from among the dependent uncertainties shown by the KF for the second contact. Finally, the direction of α is chosen to establish another new contact. For this contact, the KF gave a final P-matrix with all elements nearly zeros. Such a P-matrix is an indication that all uncertainties are completely determined.

These simulation results prove that the contacts can be randomly chosen from among the dependent uncertainties indicated by the P-matrices until the KF indicates a P-matrix showing the completion of uncertainty determination with all its elements close to zero. See the section under *Simulation Results* for results.

6. RATIONALE OF THE STRATEGY

In reference [1], a Singular Value Decomposition (SVD) of the state covariance matrix was used to gain information about the state observability of the system. The comparison of the singular values is only possible in a qualitative way. In the random contact strategy presented in this paper, we only need to look at the error covariance matrix to indicate the direction of the dependencies.

Figure 3 shows a vector state representation of the dependent variables α, β, and γ. Instead of being able to observe the three independent directions of the uncertainties, the KF can observe one direction such as $(\alpha + \beta + \gamma)$ as shown in Figure 3. Then the KF is said to be able to determine a dependency in the α, β, γ space rather than the independent vectors α, β, and γ. In this particular case, only the sum of α, β, and γ is known in a contact situation. The covariance matrix will show the dependencies of the uncertainties as,

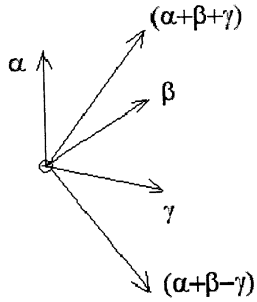

Fig. 3. Vector space representation of three dependent uncertainties.

$$\alpha + \beta + \gamma = \mathbf{C}_1 \tag{10}$$

Knowing that regardless of the joint distribution of two random variables, we can always find a change of coordinates in which the covariance is zero and the variances in this new coordinate system are either a maximum or minimum.[19] Our aim is to find new contact situations that will enable us to place the covariance matrix approach zero.

With a random process, another contact situation is produced with a known relationship with the previous contact situation. In the 2-D case described here a change in β can be obtained by turning the end-effector by 180°. The relationship that could be identified using the KF is:

$$\alpha' + \beta' + \gamma' = \boldsymbol{C}_2 \tag{11}$$

with $\beta = -\beta'$

The idea is to establish as many relationships as may be necessary to be able to determine the uncertainties. As the process continues the Estimation Error Covariance Matrix will give an indication as soon as a particular uncertainty is determined by setting its variance to zero. For example, if β has been determined we can avoid exciting the system in that direction. The vector space to be considered is shown in Figure 4. The relationship is:

$$\alpha'' + \gamma'' = \boldsymbol{C}_3 \tag{12}$$

We could find for the two uncertainties by taking the reverse of the frictional angle γ as the fourth contact situation. This will then give the relationship

$$\alpha''' + \gamma''' = \boldsymbol{C}_4 \tag{13}$$

where $\gamma'' = -\gamma'''$. Solving (12) and (13), all the dependent uncertainties of the contact situation can be found.

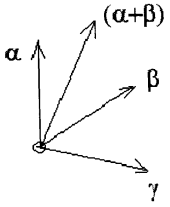

Fig. 4. Vector space representation of two dependent uncertainties.

https://doi.org/10.1017/S0263574700002903 Published online by Cambridge University Press

7. SIMULATION RESULTS

In order to simulate the uncertainty problem, the set-up shown in Figure 1 was designed. This consists of a six axes force sensor, a gripper, and a cylindrical peg. The peg is then placed in contact with the surface and the random contact sequences were carried out to test its validity.

The measurement model used to describe the first contact situation is given below. This equation considers the presence of friction in the system by including the friction angle (γ).

$$\begin{aligned} F_x &= 0 \\ F_y &= -F\cos(\alpha+\beta+\gamma) \\ F_z &= -F\sin(\alpha+\beta+\gamma) \\ M_x &= -F\sin(\alpha+\beta+\gamma)(r-y) \\ &\quad + F\cos(\alpha+\beta+\gamma)(0.1285+z) \\ M_y &= 0 \\ M_z &= 0 \end{aligned} \tag{14}$$

The uncertainties to be determined are the contact force (F), the contact angle between the peg and the surface (α), the grasping angle error (β), the friction angle (γ), and y and z which accounts for the actual coordinates displacements of the contact point with respect to the ideal point. The true values used are $\alpha = 38°$, $\beta = 7°$, $\gamma = 3°$ $y = 0.0093$m, $z = 0.0074$ m.

Sets of forces were then acquired at a sampling rate of 1000 Hertz. These forces are then processed using the KF. The results are shown in Figure 5. The estimated values are $\alpha = 37°$, $\beta = 6.02°$, and $\gamma = 4.02°$ which deviates from the true values. The resulting error covariance matrix (P_i) for the first contact is shown below. By looking at the P_i matrix, the dependencies exist in the corresponding state variables with large values. The dependent state variables are α, β, and γ which accounts for the error in estimation.

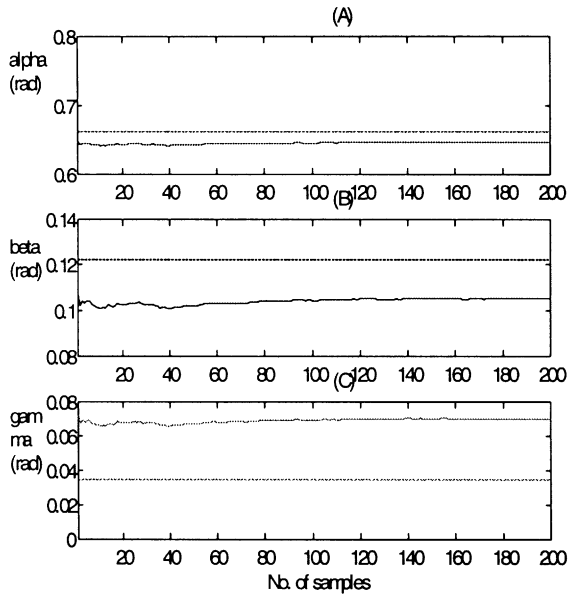

Fig. 5. Initial contact results (1st sequence).

$$P_i = \begin{array}{c} \begin{matrix} \boldsymbol{F} & \alpha & \beta & \gamma & \boldsymbol{y} & \boldsymbol{z} \end{matrix} \\ \begin{bmatrix} 0.0001 & 0.0000 & 0.0000 & 0.0000 & 0.0000 & 0.0000 \\ 0.0000 & \mathbf{0.0203} & \mathbf{-0.0102} & \mathbf{-0.0102} & 0.0000 & 0.0000 \\ 0.0000 & \mathbf{-0.0102} & \mathbf{0.0203} & \mathbf{-0.0102} & 0.0000 & 0.0000 \\ 0.0000 & \mathbf{-0.0102} & \mathbf{-0.0102} & \mathbf{0.0203} & 0.0000 & 0.0000 \\ 0.0000 & 0.0000 & 0.0000 & 0.0000 & 0.0000 & 0.0000 \\ 0.0000 & 0.0000 & 0.0000 & 0.0000 & 0.0000 & 0.0000 \end{bmatrix} \end{array} \tag{15}$$

Without carrying out a Singular Valve Decomposition, we now create a new contact by rotating the peg by 180° in the direction of β. The new measurement equation for the contact situation is shown below.

$$\begin{aligned} F_x &= 0 \\ F_y &= F'\cos(\alpha'+\beta'+\gamma') \\ F_z &= -F'\sin(\alpha'+\beta'+\gamma') \\ M_x &= F'\sin(\alpha'+\beta'+\gamma')(r-y') \\ &\quad - F'\cos(\alpha'+\beta'+\gamma')(0.1285+z') \\ M_y &= 0 \\ M_z &= 0 \end{aligned} \tag{16}$$

Using these equations and the force measurement data, the resulting estimation is shown in Figure 6. Looking at the error covariance matrix, P_{ip}, the three uncertainties α, β, and γ are still unidentified.

$$P_{ip} = \begin{bmatrix} 0.0001 & 0.0000 & 0.0000 & 0.0000 & 0.0000 & 0.0000 \\ 0.0000 & \mathbf{0.0534} & \mathbf{-0.0254} & \mathbf{-0.0279} & 0.0007 & -0.0007 \\ 0.0000 & \mathbf{-0.0254} & \mathbf{0.0170} & \mathbf{0.0085} & -0.0004 & 0.0005 \\ 0.0000 & \mathbf{-0.0279} & \mathbf{0.0085} & \mathbf{0.0195} & -0.0002 & 0.0002 \\ 0.0000 & 0.0007 & -0.0004 & -0.0002 & 0.0000 & 0.0000 \\ 0.0000 & -0.0007 & 0.0005 & 0.0002 & 0.0000 & 0.0000 \end{bmatrix} \tag{17}$$

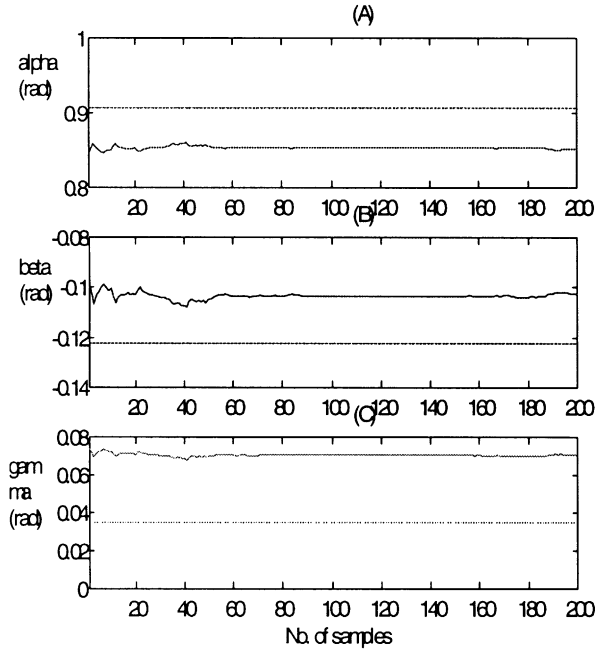

Fig. 6. Second contact. This was established after turning the gripper by 180° (1st sequence).

https://doi.org/10.1017/S0263574700002903 Published online by Cambridge University Press

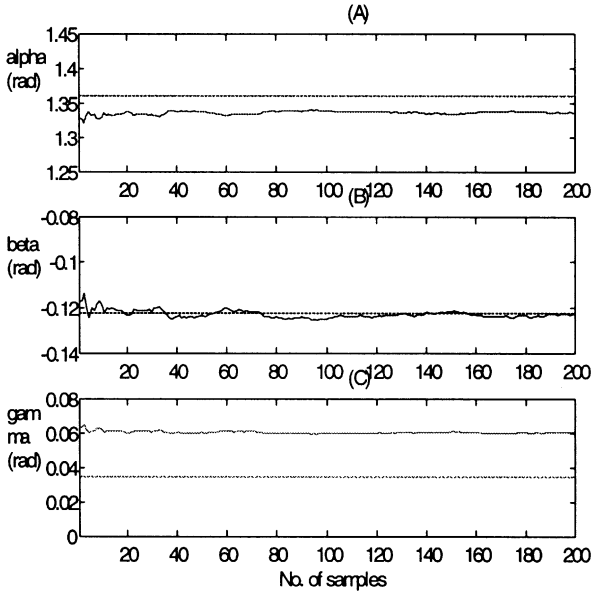

Fig. 7. Third contact by changing the angle of α. Note that β has converged. (1st sequence).

To proceed further, a change in the angle α is made. Its value is changed by 26 degrees while keeping all the other uncertainties constant (any angle changes from 15 to 34 degrees gave good convergence). We could now accurately estimate the value of β as can be seen in Figure 7 and the P_{if} matrix. The resulting P-matrix is,

$$P_{if} = \begin{bmatrix} 0.0001 & 0.0000 & 0.0000 & 0.0000 & 0.0000 & 0.0000 \\ 0.0000 & \mathbf{0.0157} & -0.0003 & \mathbf{-0.0154} & 0.0000 & 0.0000 \\ 0.0000 & -0.0003 & 0.0002 & -0.0001 & 0.0000 & 0.0000 \\ 0.0000 & \mathbf{-0.0154} & -0.0001 & \mathbf{0.0153} & 0.0000 & 0.0000 \\ 0.0000 & 0.0000 & 0.0000 & 0.0000 & 0.0000 & 0.0000 \\ 0.0000 & 0.0000 & 0.0000 & 0.0000 & 0.0000 & 0.0000 \end{bmatrix} \quad (18)$$

By reversing the direction of the velocity both β and γ is found. The graphical results of Figure 8 will confirm the validity of the identification process. We could also verify the identification by looking at the P_{ir} matrix given below.

$$P_{ir} = \mathbf{10}^{-3} \begin{bmatrix} 0.0406 & 0.0188 & -0.0164 & 0.0000 & 0.0006 & -0.0009 \\ 0.0188 & 0.1930 & -0.1893 & -0.0102 & 0.0021 & -0.0048 \\ -0.0164 & -0.1893 & 0.1863 & -0.0102 & -0.0021 & 0.0048 \\ 0.0000 & -0.0012 & -0.0012 & 0.0001 & 0.0000 & 0.0000 \\ 0.0006 & 0.0021 & -0.0021 & 0.0000 & 0.0000 & -0.0001 \\ -0.0009 & -0.0048 & 0.0048 & -0.0000 & 0.0001 & 0.0002 \end{bmatrix} \quad (19)$$

As could be seen from the final error covariance matrix (P_{ir}), the dependencies that were present in the first contact are diminished. The unobservable quantities are all identified as indicated both by the final error covariance matrix and the graphical comparison of the estimated values and the true values in Figure 8. This indicates the effectiveness of using the procedure to successfully identify the unobservable quantities. In order to verify the effectiveness of the random contact procedure, a second random contact sequence was carried out. This too was based on the

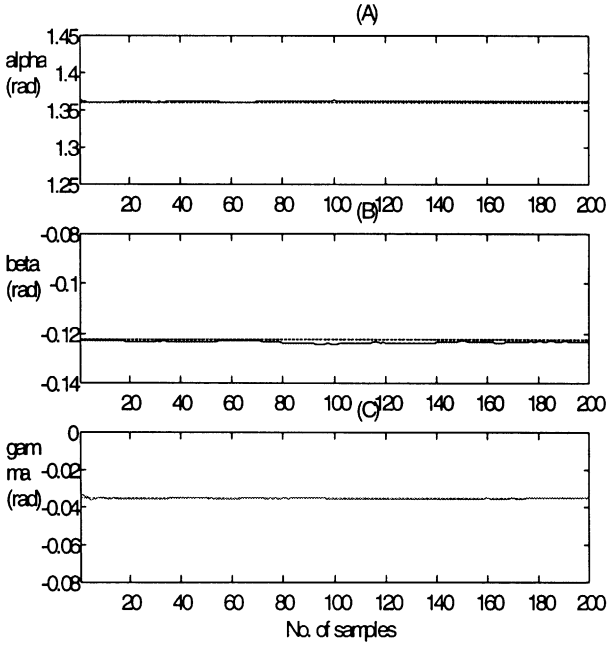

Fig. 8. Final contact established by reversing the direction of friction. All uncertainties have converged (1st sequence).

unobservable direction to form the next contact but in a different order to the first random contact sequence. The result of the procedure could be seen in Figures 9 to 12. This procedure followed (1) first contact, (2) reversing the direction of friction, (3) turning by 180°, and (4) changing the value of α. The error covariance matrix followed a similar path as the first procedure indicating a good estimate of the uncertainties.

The need to identify the relationship between the three dependent uncertainties using Singular Value Decomposition was eliminated. Instead we only need change the contact situation in the direction of the unobservable quantities in a random manner. It is shown above the

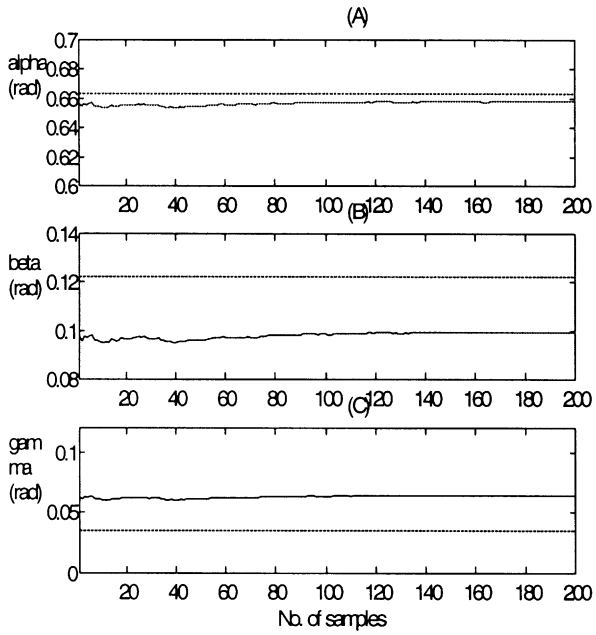

Fig. 9. Initial contact results (2nd sequence).

https://doi.org/10.1017/S0263574700002903 Published online by Cambridge University Press

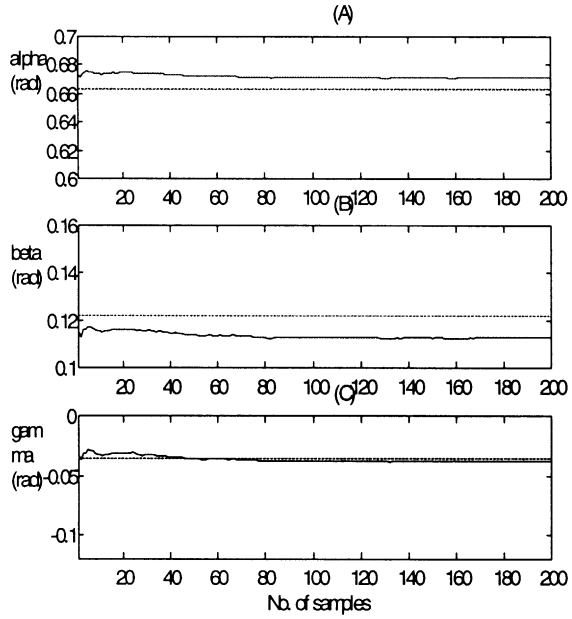

Fig. 10. Second contact established by reversing the direction of friction. Note that γ has converged (2nd sequence).

movement in either of the two random contact procedures led to the same final complete solution.

8. EXPERIMENTAL RESULTS

The method was implemented on a PUMA 560 robot. The set-up includes a crash protector, a force sensor, a thin block of metal to introduce a grasping error and a cylindrical peg. The experimental set-up is shown in Figure 13 and 14. The grasping and contact uncertainties were found using the second random procedure described earlier. The peg was slowly moved downward and the random contact sequence was implemented.

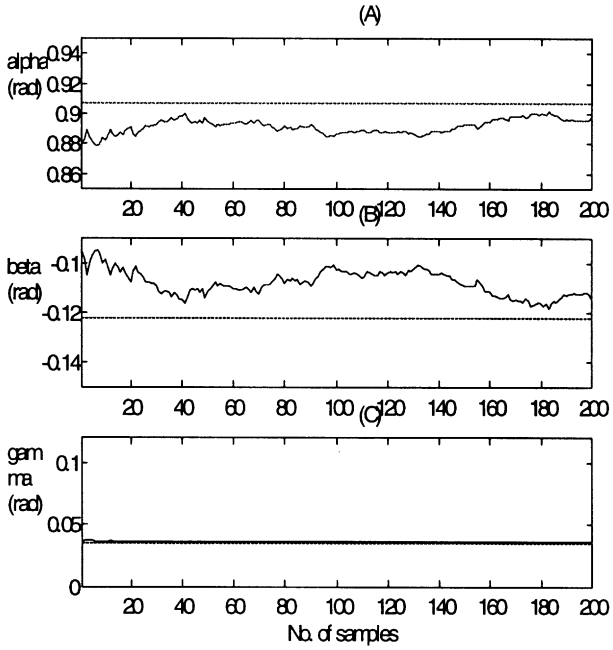

Fig. 11. Third contact. This was established after turning the gripper by 180° (2nd sequence).

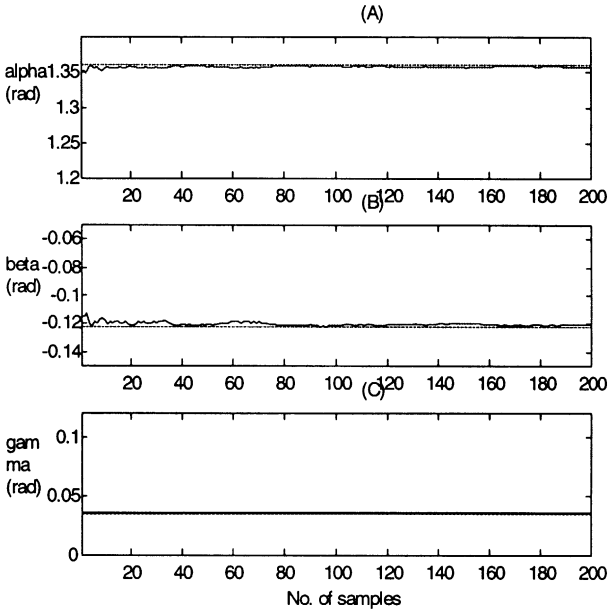

Fig. 12. Final contact by changing the angle of α in contact. All uncertainties have converged (2nd sequence).

In the experiment, the true values of the unobservable quantities in the first contact situation are $F = 5$, $\alpha = 78°$, $\beta = 5°$, $\gamma = 12°$ (experimentally determined, taken to be the angle of repose), $y = 0.0077$ m, and $z = 0.00948$ m. The value of γ is only an approximation based on an experiment done to find the friction angle of the peg-surface contact.

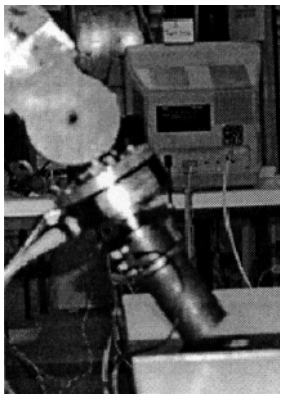

Fig. 13. Initial experimental contact situation.

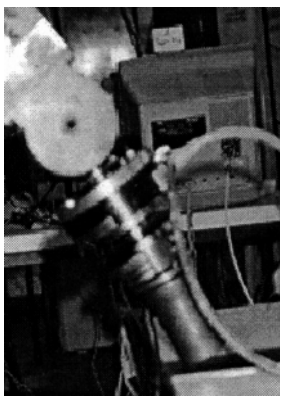

Fig. 14. 180° peg turn from initial contact.

https://doi.org/10.1017/S0263574700002903 Published online by Cambridge University Press

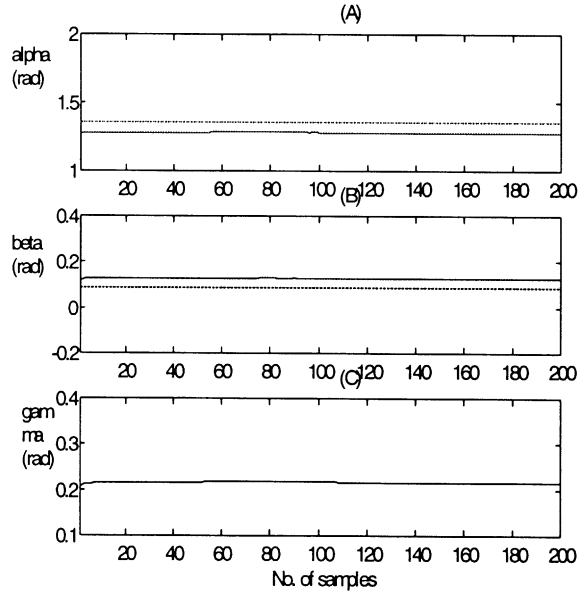

Fig. 15. Initial contact results (experimental).

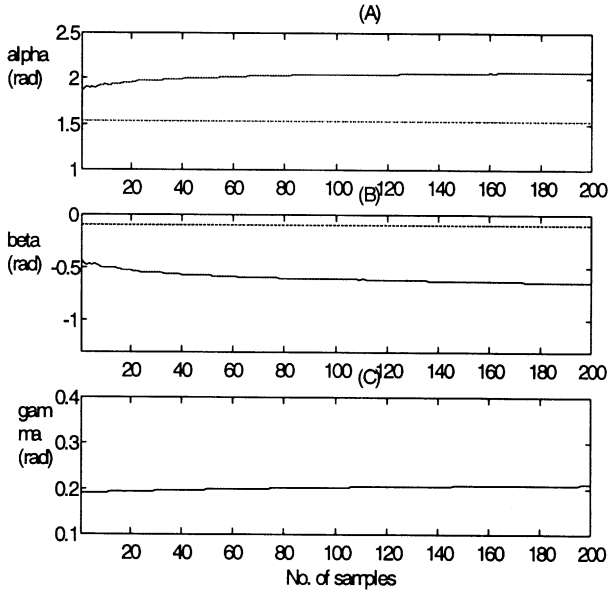

Fig. 17. Third contact. This was established after turning the gripper by 180° (experimental).

While the values of α, β, y, and z, were based on the geometry of the peg and the contact configuration.

The experimental results are found in Figures 15 to 18. Using the second random contact sequence the dependent uncertainties were found. The true values of the last contact situation are $F = 5$N, $\alpha = 43°$, $\beta = 5°$, $\gamma = 12°$, $y = -0.0075$ m and $z = 0.0055$ m. While the final values of the uncertainties are $F = 5.137$N, $\alpha = 0.7431$ (42.57°), $\beta = -0.1026(-5.87°)$, $\gamma = 0.2168$ (12.42°), $y = -0.0061$ m and $z = 0.0038$ m. The final P = matrix after implementing the random contact strategy is shown in equation 20. It proved the validity of the random excitation procedure in finding the unobservable uncertainties. There is a slight discrepancy in the values of the displacement. This may be due to some flexibility present in the system. Further, there may be modelling inaccuracies present.

$$P_{iw} = 10^{-4} \begin{bmatrix} 0.1308 & 0.0780 & -0.0740 & -0.0051 & 0.0004 & -0.0026 \\ 0.0780 & 0.1389 & -0.1326 & -0.0061 & 0.0008 & -0.0025 \\ -0.0740 & -0.1326 & 0.1270 & 0.0057 & -0.0008 & 0.0025 \\ -0.0051 & -0.0061 & 0.0057 & 0.0007 & 0.0000 & 0.0001 \\ 0.0004 & 0.0008 & -0.0008 & 0.0000 & 0.0000 & 0.0000 \\ -0.0026 & -0.0025 & 0.0025 & 0.0001 & 0.0000 & 0.0001 \end{bmatrix} \quad (20)$$

9. CONCLUSION

The unobservable uncertainties of the robotic contact can be determined by carrying out a sequence of contacts. The contacts are selected from among the directions of dependencies of the uncertainties. The estimation error

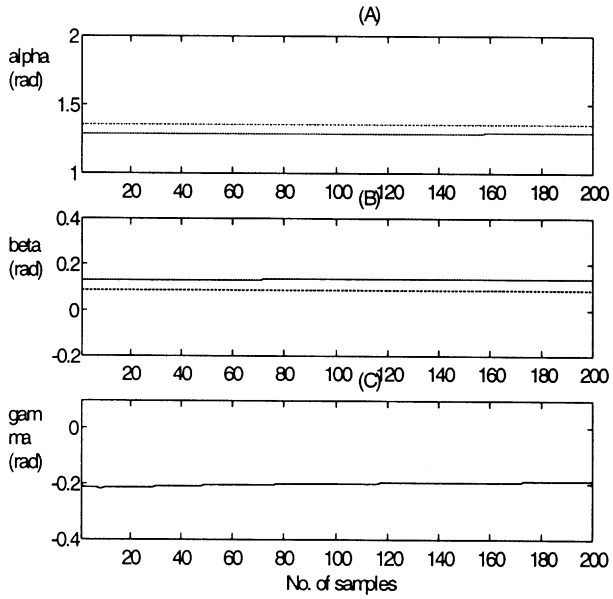

Fig. 16. Second contact established by reversing the direction of friction. Note that γ has converged (experimental).

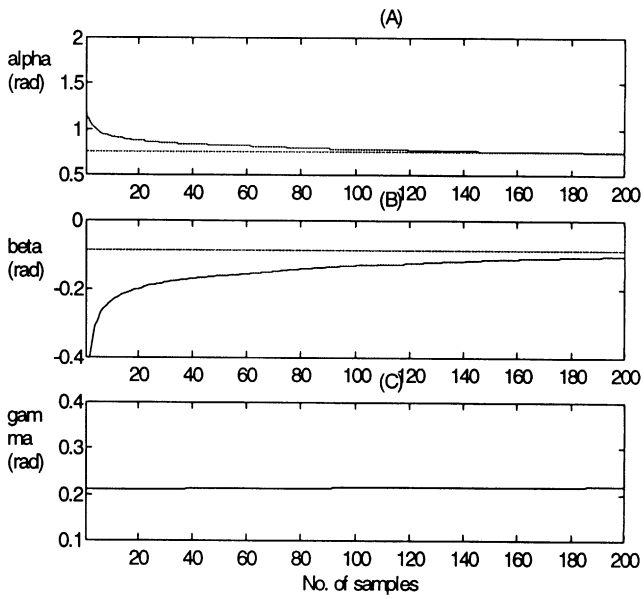

Fig. 18. Final contact by changing the angle of α in contact. All uncertainties have converged (experimental).

https://doi.org/10.1017/S0263574700002903 Published online by Cambridge University Press

covariance matrix of the KF shows the dependent uncertainties. The results of the simulation proved our ability to randomly pick and excite one of the unobservable directions to form the next contact. That is, the order in which the unobservable directions are excited is unimportant. The method does not require a Singular Value Decomposition to be carried out. When this method is implemented in an experiment, reasonably accurate results were obtained. The minor inaccuracies may be attributed to measurement model inaccuracies and the non-zero twist vector. Note that the twist vector has not been included in the observations. Only the wrench vector has been used. During the experiment, every attempt has been made to keep the twist vector close to zero so that the validity of the method can be verified. If the twist can be accurately measured, it can be incorporated in the measurement model. These results will be augmented in future studies incorporating execution of multiple unobservable directions in a single contact change.

References

1. J. Katupitiya, S. Dutre, S. Demey, J. De Geeter, H. Bruyninck and J. De Schutter, "Estimating Contact and Grasping Uncertainties Using Kalman Filters in Force Controlled Assembly", *Proceedings of the IEEE/RSJ International Conference on Intelligent Robots and Systems* (1996) pp. 696–703.
2. J. De Schutter et al., "Estimating First Order Geometric parameters and Monitoring Contact Transitions during Force-Controlled Compliant Motion, *Int. J. Robotics Research* **18**, No. 12, 1161–1184 (1999).
3. H. Cho, H. Warnecke and D. Gweon, "Robotic assembly: a synthesising overview", *Robotica* **5**, Part 153–165 (1987).
4. J. Merlet, "Force Feedback Control in Robotic Tasks", *Intelligent Robotic Systems* (Marcel Dekker, 1991), pp. 283–311.
5. H. Qiao, B. Dalay and R. Parkin, "Robotic Peg-hole Insertion Operation using a Six Component Force Sensor", *Proc. Instn. Mech. Engrs,* **207**, 289–306 (1993).
6. M. Blauer and P. Belanger, "State and Parameter Estimation for Robotic Manipulators Using Force Measurements", *IEEE Transaction on Automatic Control* **32**, 1055–1066 (Dec. 1987).
7. H. Miyaguchi and K. Iwama, "A Strategy of Assembly Task Execution in the Presence of Uncertainties", *IEEE International Conference on Robotics and Automation* (1994) **Vol. 2**, pp. 1456–1461.
8. A. Bicchl, J. Salisbury and D. Brock, "Contact Sensing from Force Measurements", *Int. J. Robotics Research* **12**, 249–262 (June, 1993).
9. P. T. Liu, F. Li and H. Xiao, "A State Decoupling Approach to Estimate Unobservable Tracking Systems", *IEEE Journal of Oceanic Engineering* **21**, 256–259 (1996).
10. S. Kou, D. Elliott and T. Tarn, "Observability of Nonlinear Systems", *Information and Control* **22**, 89–99 (1973).
11. A. Abur and A. Exposito, "Detecting Multiple Solutions in State Estimation in the Presence of Current Magnitude Measurements", *IEEE Transaction on Power Systems* **12**, 370–375 (1997).
12. S. Hammel and V. Aidala, "Observability Requirements for Three-Dimensional Tracking via Angle Measurements", *IEEE Transaction on Aerospace and Electronic Systems* **21**, 200–207 (1985).
13. W. Dayawansa, B. Ghosh, C. Martin and X. Wang, "A necessary and sufficient condition for the perspective observability problem", *Systems and Control Letters* **25**, 159–166 (1995).
14. A. Gelb, *Applied Optimal Estimation* (The MIT Press, 1974).
15. Y. Bar-Shalom and X. Li, "*Estimation and Tracking Principles, Techniques and Software"* (Artech House, 1993).
16. J.M. Hollerback and D.M. Lockhorst, "Closed-loop Kinematic Calibration of the RSI 6-DOF Hand Controller", *IEEE Transactions on Robotics and Automation* **11**, No. 3, 352–359 (June, 1995).
17. C.W. Wampler, W. Charles, J.M. Hollerbach and T. Arai, "Implicit Loop Method for Kinematic Calibration and its Application to Closed-chain Mechanisms", *IEEE Transactions on Robotics and Automation* **11**, No. 5, 710–724 (1995).
18. C.C. Iurascu and F.C. Park, "Geometric Algorithms for Closed Chain Kinematic Calibration", *IEEE International Conference on Robotic and Automation,* **Vol. 3**, pp. 1752–1757, (1999).
19. P. Liebelt, *An Introduction to Optimal Estimation* (Addison-Wesley Publishing Company, 1967).

https://doi.org/10.1017/S0263574700002903 Published online by Cambridge University Press